Arabian Journal of Geosciences (2021) 14:1474
https://doi.org/10.1007/s12517-021-07794-w

ORIGINAL PAPER

Space-time hydrochemical variations and water quality of Euphrates river

Bayan Muhie Hussien[1] · Nabeel Fawzi Lattoofi[2] · N. M. Abd-alghafour[3] · Rasim Farraj Muslim[1] · Tahseen Zaidan[1] · Marwan Mahmood[1]

Received: 8 October 2020 / Accepted: 20 May 2021

Abstract

The study of hydrochemical variations and water quality assessment of the Euphrates river was performed in eight water points and two rainfall sites, during a boundary condition of rainy weather. The hydrochemical variations are determined, using the analysis results of 14 physico-chemical variables in 26 water samples. The study examined the depletion and attenuation processes during a rainstorm and the re-enrichment of the concentrations after rain event by using the statistical information of the major ions (HCO_3^-, SO_4^{-2}, Cl^-, Mg^{+2}, Ca^{+2}, Na^+, and K^+). The lowest values of Cl^-, $SO4^{-2}$ were observed (94.7 and 202 mg/L) during the rain storm period, while the highest value of Cl^- (114 mg/L) and SO_4^{-2} (254 mg/l) were recorded before and after rain storm, respectively. The values K^+, Na^+, Mg^{+2}, and Ca^{+2} are (3.3, 73.5, 35.8, and 83 mg/L). The hydrogeochemical indices confirm the role of irregular processes of chemical balance resulting from the propagation of mixing, ion exchange, and water-rock interaction between river and rainstorm water during high flow period. The results that derived from water quality assessment indicate that there are no serious geogenic pollution cases, with the absence of thermal pollution sources which is degradation of water quality by any process that changes ambient water temperature such as domestic sewage, hot springs, and soil erosion that forms serious impact on the biological diversity of the Euphrates water system. The total dissolved solids (TDS) and electrical conductivity (EC) measurements ranging from 484 to 778 mg/L and from 770 to 985 μScm^{-1}, respectively.

Keywords Water quality · Hydrochemical facies · Euphrates river · Rainfall impact

Introduction

Since 70 years, the mean annual of temperature, precipitation, and evaporation in the study area (Fayyadh et al. 2016) ranged between 20-22 °C, 125-100 mm, and 1900-2000 mm, respectively. According to the tectonic setting, the course of the Euphrates river falls within the scope of the Transversal Fault System, represented by the Samarra-Amij Fault, which impact with Abu-Jir Fault on the direction of the river. Figure 1 indicated the Oligocene, Miocene, and Quaternary deposits are exposed within the river basin. The most important formations of Oligocene are Sheikh Alas formation, which appears in al-Baghdadi region and on the western edges of the riverbed. Shurao formation, which exposed in Horan valley and deep shore edges of the Euphrates river between Haditha and Baghdadi, especially in the confluence of seasonal valleys with the riverbeds (Sessikian and Mohammed 2007; Amiri and Berndtsson 2020).

Miocene deposits occupy the majority of the study area, which consists of Euphrates formation (Lower Miocene). This formation consists of dolomitic limestone with fractures as well as layers of basal conglomerates. Fatha formation of middle Miocene consists of gypsum, anhydrite, salts, and claystones. The two formations are located on the left side of the river, while Euphrates formation is exposed west of the river between Haditha and Baghdadi. Quaternary deposits consist of Early, Middle, Late, and Holocene sediments appear in the sections on both sides of the Euphrates river,

Responsible Editor: Broder J. Merkel

✉ N. M. Abd-alghafour
nabeel.ma@uoanbar.edu.iq

[1] Department of Ecology, College of Applied Sciences-Hit, University Of Anbar, Anbar, Iraq

[2] Department of Physics, College of Science, University Of Anbar, Anbar, Iraq

[3] Iraqi Ministry of Education, Al-Anbar, Biophysics Department, College of Applied Sciences-Hit, University Of Anbar, Anbar, Iraq

Published online: 23 July 2021

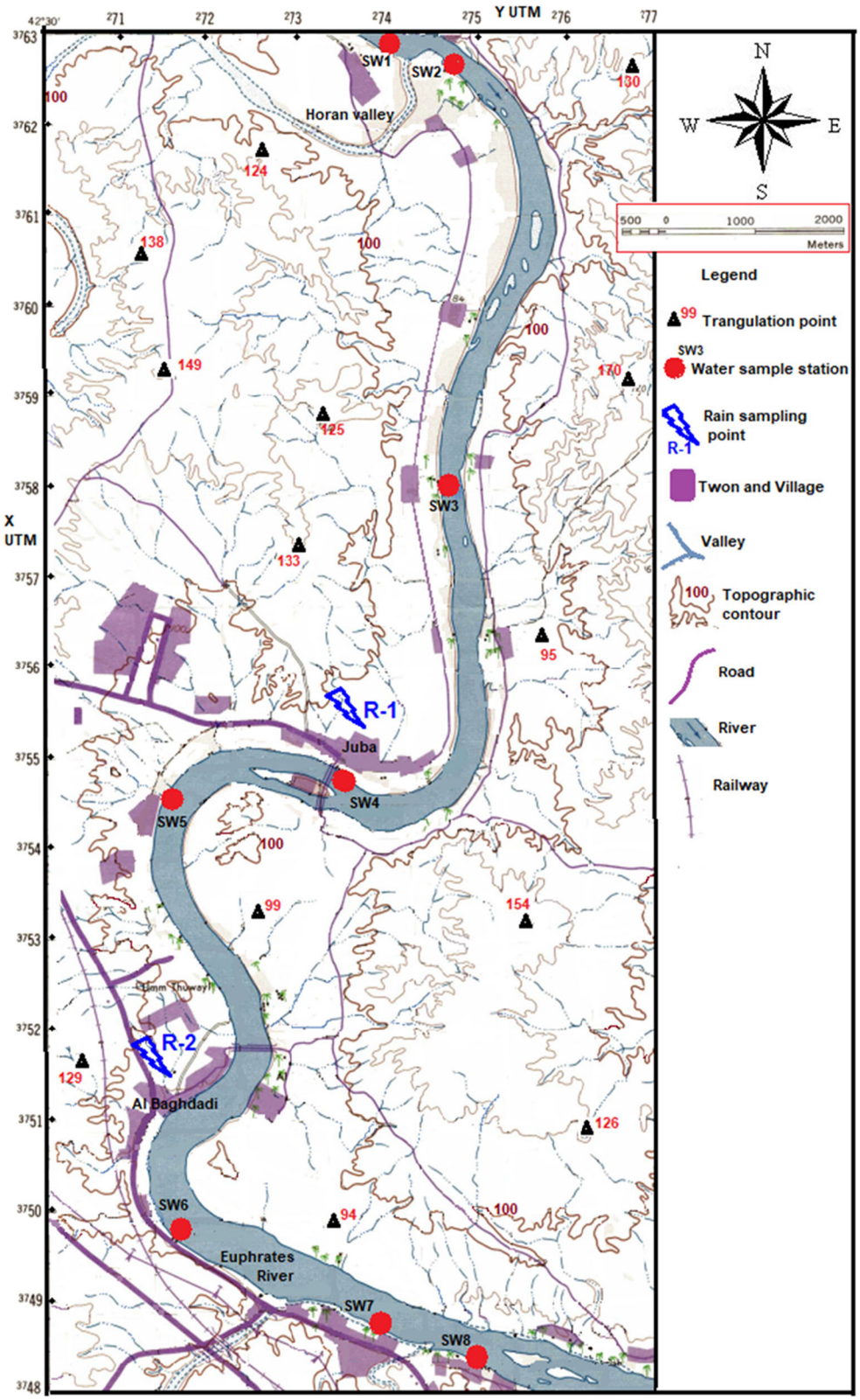

Fig. 1 Map of monitoring sites within the study region

including river terraces (Tyracek 1981), consisting of gravel and sand, as well as flood, river shoulders, and valley sediments. The thermal pollution occurs due to several causes such as domestic sewage which is discharged into rivers, lakes, canals, or streams without treating the waste. The temperature of municipal water sewage is normally high than

receiving water. The natural causes like hot springs can trigger warm lava to raise the temperature of water bodies. Soil erosion is another major factor that causes thermal pollution. Consistent soil erosion causes water bodies to rise, making them more exposed to sunlight. The high temperature could prove fatal for aquatic biomes as it may give rise to anaerobic conditions.

A previous study that determined the hydrochemical properties of Euphrates river was achieved through the monitoring system during the period 1997-2000 (Al-Jabbari et al. 2002). Al-Janabi (2008) examined the factors of environmental impact on water quality of the Euphrates river using remote sensing and laboratory analysis through monitoring and linkage between two techniques during the water year. Issa et al. 2014) utilized monthly water discharge measurements for 15 stream flow monitoring points within Iraq on the Tigris-Euphrates rivers. The analysis indicated that Iraq receives yearly 70.92 km^3 of water, 45.4 and 25.52 km^3 from River Tigris and Euphrates, respectively. The entire volume of water in the Euphrates river comes outside the Iraqi borders. Annual decrease of the water inflow was 0.1335 km^3/year for Tigris and 0.245 km^3/year for Euphrates. This implies that the annual percentage reduction of inflow rates for the two rivers was 0.294% and 0.960%, respectively. While Fayyadh et al. (2016) study dealt with the hydrologic system classification of Euphrates river based on geological, hydro meteorological, and hydrochemical phenomena, into three subsystems. The hydrochemical properties of Euphrates river waters are determined by using the analysis results of 21 physicochemical variables during the water year (2008). The interpretation of the hydrochemical phenomena is achieved in accordance with the statistical results of Polynomial Regression Statistic, calculating the coefficient of variation among the physicochemical components of the water terminating by 14 models. Al-Hamdani et al. (2012) examined the sources of ions and trace elements in river water between Qaem City and Al-Baghdadi City using statistical techniques. The presumptive statistical and relevant difference findings were utilized to evaluate the differences in water components along the Euphrates river valley. The study also determined the natural hydro-geochemical effectiveness within the ecosystem of Euphrates river and Haditha lake, to prove and reaches the other related environmental effectiveness, which affect the hydrologic system, such as ground water, waste water, and irrigation drained water. Rana et al. (2018) examined the pollution levels of leachate derived from three non-engineered landfill sites located in the Northern India and the potential impacts of groundwater contamination. The values of the Leachate Contamination Index for landfill sites of Chandigarh, Mohali, and Panchkula are 26.1, 27, and 27.8, respectively. The results indicated that the leachate generated is contaminated. The measurement of the WQI over the various downwind distances from the pollution sites showed that the groundwater quality improved with a rise in width from the downwind. Sharma et al. (2020) evaluated the pollution level of leachate in the vicinity of four non-engineered dump sites in the study regions of Solan, Mandi, Sundernagar, and Baddi in Himachal Pradesh, India, and its effects on surrounding groundwater. For the samples obtained from four research areas, the study compiled the physicochemical characterization of leachate and groundwater, heavy metal analysis, leachate contamination index, water quality index, and heavy metal emission index. The LPI of the samples were calculated to be 17, 17, 14, and 22, respectively, which exceeded the allowable values and suggested high levels of toxicity. The water quality indices (WQI) has been shown to be of moderate and average quality for groundwater samples collected from sources closer to the immediate vicinity of dumpsites, but groundwater quality has improved with the distances from the dumpsites. Vasistha and Ganguly 2020a, 2020b) examined the characteristics of two lakes situated in close vicinity to each other in determining the location of the lakes based on Designated Best Use (DBU) criteria for optimum use. For the determination of water quality indices (WQI), the analysis used about twenty parameters tested experimentally. In presenting the total WQI of the lakes, the WQI was calculated to be depth wise and a weighted average approach was used to represent the true water quality based on depth wise assessment. Vasistha and Ganguly 2020a, 2020b) was offered a summary and critically assesses the literature on all aspects of water quality to provide insight into the different methods and strategies used for full monitoring and management of water quality. The water quality takes into account the physical, chemical, and biological criteria for determining and preserving water quality. Different parameters, such as TDS, pH, temperature, BOD, COD, phosphorus, DO, phytoplankton, bacteria, SO_4, Ca, Na, Mg, NO_3, NO_2, and NH_4, were measured and compared to the normal limits prescribed by agencies such as CPCB, WHO, and BIS.

The current research have evaluated the water of the Euphrates river for environmental purposes related to aquatic life and the other purposes, based on the hydrochemical properties of the Euphrates river (Al Baghdadi sector) within the scope of the second hydro-meteorological system, in terms of mixing-dilution and/or enrichment processes related to the river condition during high and base flow stages. The most significant target of this study is to determine the hydrochemical phenomena of the Euphrates river in a sector comes after man-made storage lake (Haditha), which changes the environment of the Euphrates from natural river system to the lake environment with high ability to assimilate various input additives like ions and trace elements. The physicochemical components found that their values were within their limits in a natural river environment and less than the prescribed limits for domestic use and human drinking purposes during rainy periods (Kamrani et al. 2016). Here, it is

necessary to understand the sources and processes directly controlling water quality and to quantify the impacts of climatic variability throughout rainstorm event, according to monitoring program plan carried out in eight pre-installed sites for water sampling.

Material and methodology

Study location

The Euphrates river runs north-south in the land with an elevation ranged between 64 and 75 m above sea level (asl) at a slope of 54 cm/km to the south. It is bordered by the shore of undulating plateau of 100-150 m (asl). A series of parallel intermittent seasonal valleys, with various discharge capacity, pour on both sides of the river, as shown in Fig. 1. The Euphrates river is the discharge zone of the groundwater on both sides at a level ranged between 64 and 80 m (asl), with bank storage conditions, where the groundwater mixed with river water in the adjacent bar sections. Figure 2 shows the flow of groundwater in the left bank is W-SW wards, whereas E-NE and SE direction on the right bank with values of hydraulic gradient ranged between 0.005 and 0.02. The fluctuation of the groundwater level was about 0.6 m. The transmissivity coefficient of the Euphrates aquifer ranged between 34 and 960 m^2/day, while the storage coefficient is 0.0176 (Al-Sudani 2018; US Environmental Protection Agency 2002). The groundwater outflow to the Euphrates river was calculated on river stage, according to the equation $Q = TIL$, using the hydraulic information of the aquifers and hydrogeologic map, as shown in Fig. 2. The amount of base and high flow discharge of the Euphrates river during the monitoring period are 21.6×10^6 and 21.92×10^6 m^3/day, respectively. Also, the amount of rainwater falling directly on the river's water is 0.112×10^6 m^3/day (Table 1).

Field and laboratory works

A monitoring program of collection water samples from the Euphrates river in 8 stations, and two rain water samples from mobile gauge within the scope of the Baghdadi region during February 2018, at three periods, including the period before rainstorm (5/2/2018), period of rainfall (16/2/2018), and the period after rainstorm (18/2/2018). Eight samples were collected for each of the study sites during the study period. The water specimens were taken at a depth of 10 cm from ten selected sites by using Shelton (1994), APHA (1998), Dunnette (1992), and USEPA (2000) procedures, which were connected to the variables monitored in this analysis. All the equipment used to collect, store, and analyze chemical components for samples was pre-cleaned using deionized water. Such cleaning and storage processes confirm that the sampling equipment does not have detectable pollutants (Shafer et al. 1997). The samples were taken by normal bucket maintained in glass bottles after collection. The coordinates are set by Garmin GPS at each sampling station. The preparations, selection/cleaning of equipments for water sampling, collection/processing of water samples, and field measurements are achieved according to the requirements and recommendations provided by Shelton (1994) and the USGS, National Field Manual for the collection of water-quality data (Wilde 2005; US Salinity Laboratory Staff (USSLS) 1954). Other parameters of water quality that are considered to influence dissolved element measurements were made (i.e., pH, suspended solids, and conductivity). The pH of the stream was measured using a standardized field pH meter before each reading, immediately. The pH and electrical conductivity (EC), dissolved oxygen (DO), biological oxygen demand (BOD), free ammonia and sodium absorption ratio (SAR), and the complete coliform organism test are included in the criteria.

River and rainwater samples were analyzed in Water Laboratory of Anbar Environment Directorate as well as physical and chemical parameters including water temperature (T), electrical conductivity (EC), and pH, were measured in situ using an OHAUS ST2100 pH-meter and OHAUS ST3100C conductivity meter, respectively. Bicarbonate (HCO_3^-) was measured by the titration method with (H_2SO_4); Ca^{+2} and Mg^{+2} were examined by EDTA complex metric titration. The K^+ and Na^+ concentration was calculated by flame photometer model (Corning 410), and Cl^- concentration was

Table 1 Euphrates river and groundwater discharge

Province	T m^2/day	Hydraulic gradient (I)	Distance along Eq. line (L) m	Groundwater outflow (Q) m^3/day	Total GW outflow (Q) m^3/day	Amount of rainstorm on river m^3/day	River discharge (Q) m^3/day
W River	497	0.009	22000	0.984×10^6	0.2127×10^6	0.112×10^6	21.6×10^6 (inflow)
E River	497	0.010	23000	0.1143×10^6			21.92×10^6 (out flow)

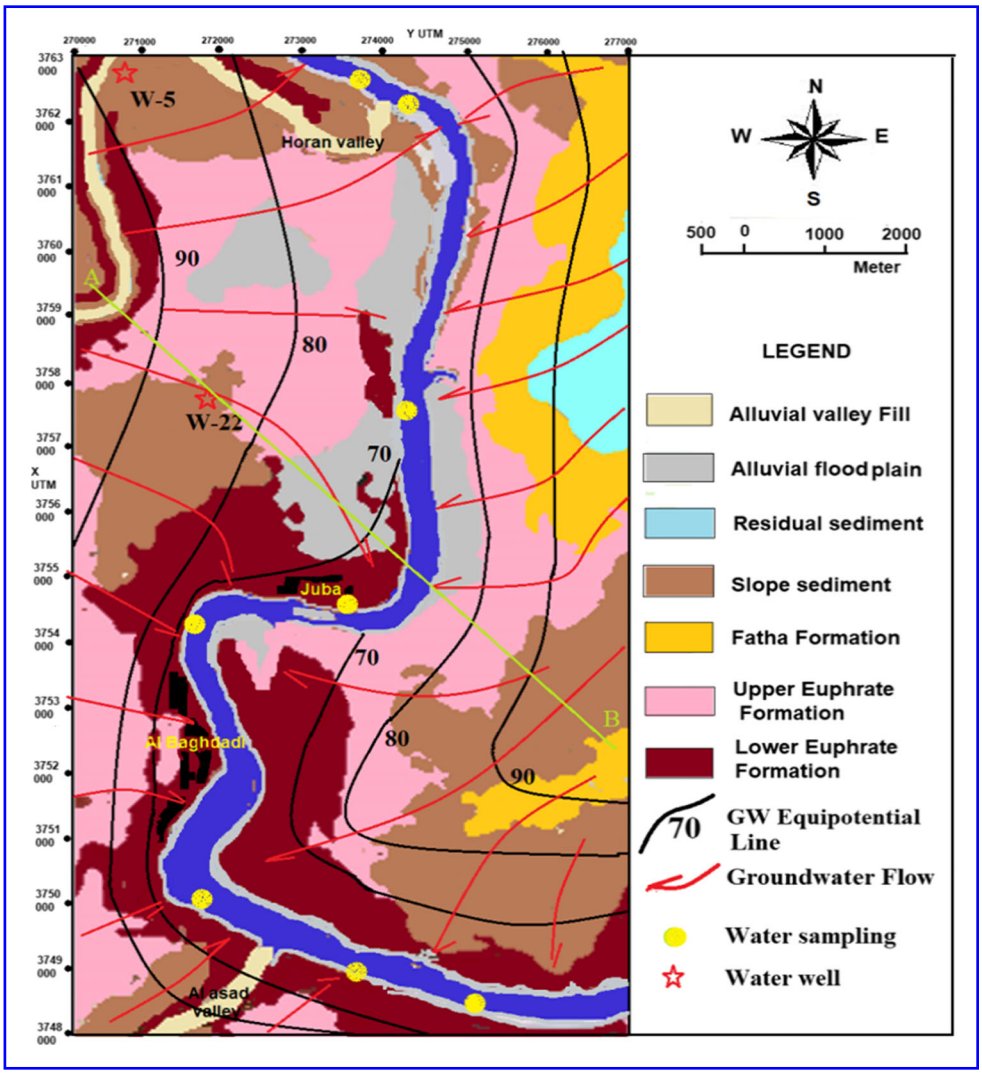

Fig. 2 Hydrogeologic map of the study region

measured by the silver nitrate method. Sulfate ($SO4^{-2}$) concentration was determined spectro-photometrically using the barium sulfate turbidity method. In this research, the geochemical modeling program AquaChem (PHREEQC) has been employed to evaluate the carbon dioxide.

Results and discussion

Hydrochemical characteristics

Daily monitored water samples from the Euphrates river during the monitored periods have pH values ranging from 7.3 to 8.2; therefor the water classified as neutral can be slightly alkaline water. The temperature of the water samples ranged from 14 to 18 °C, which classifies as cold water (Matthess 1982). The water temperature fluctuation indicates absence of any thermal pollution along the river flow path. Euphrates river, characterized by fresh water type, referring to the TDS classification (Todd and Mays 2005; Collin's 1975), where TDS values and EC measurements ranging from 484 to 778 mg/L and from 770 to 985 μScm^{-1}, respectively. These values showed the lowest mean value during a rain storm in all locations of sampling. This takes place because TDS depends on the concentration of dissolved ions. Groundwater chemistry depends on a variety of factors, such as general geology, the degree of chemical weathering of the different forms of rock, the consistency of water recharge, and inputs from sources other than the contact between water and rock (Nakhaei et al. 2016). Probably groundwater flow throughout evaporitic rocks has caused the increment of the chloride and sulfate concentration (Esmaeili-Vardanjani et al. 2015).

The Euphrates water is unsuitable for direct industrial purposes and classified as very hard water depending on H_T classification (Hem 1989), with a total hardness value ranged from 244 to 369 mg/L. Low concentrations of dissolved carbon dioxide CO_2 (g) and total carbon (TC) with same pattern trend were observed in the water samples during the monitoring

period, which ranges from 4.3 to 6.5 mg/L and from 26.5 to 33.4 mg/L, respectively.

For anions, the lowest mean values of Cl^{-}, SO_4^{-2} were observed during the rain storm period, except for HCO_3^{-}, detected before rain storm period, and their values are 94.7, 202, and 121 mg/L for Cl^{-}, SO_4^{-2}, and HCO_3^{-}, respectively. While the highest mean value of Cl^{-} (114 mg/l), SO_4^{-2} (254 mg/L), and HCO_3^{-} (137.7 mg/L), were recorded before, after, and during rain storm, respectively, that originated from the dissolution process (Siegel 2002) on the limestone and dolomite bedrock of Euphrates river. High chloride concentrations can also be due to excessive release of Waste water near the sampling places (Amiri et al. 2014). The lowest mean values of cations were observed during the rain storm period, except for Na, detected before rainstorm period, and their values are 3.1, 67.2, 31.7, and 62.5 mg/L for K^{+}, Na^{+}, Mg^{+2}, and Ca^{+2}, respectively. Their highest mean values were recorded before rainstorm except for Na that detected after rain storm. The values of K^{+}, Na^{+}, Mg^{+2}, and Ca^{+2} are 3.3, 73.5, 35.8, and 83 mg/L, respectively. The observed variability in major ion concentration originated to the mechanism of mixing related to ground water seepages and/or sewage water from Baghdad to Juba City, dilution by rain water and dissolution process with the river bed rock, followed by recovery behavior of river in the state of base flow. Figure 3 shows the spatial distribution of anions and cations percent and their variations for each observed site and river flow direction during (16/2/2018), after (18/2/2018), and before the rain storm (5/2/2018). In general, cationic and anionic concentrations are controlled by dissolution, weathering, and base-exchange processes in groundwater (Amiri et al. 2020). Chemical composition reliability was checked using the charge balance method (Fitts 2002). Table 2 characterized the chemical analyses of anions, cations, total dissolved solids (TDS), total hardness, total carbon, dissolved carbon dioxide gas, and field measurements.

Influences on water quality during storm flow

The hydrochemical deductions can be made from data variability in concentrations dominated by daily variation to provide an indication of trends during rain event. The River water quality shows rapid responding to rainstorm events which indicated by obvious physico-chemical and river discharge fluctuations. The measured data of 14 variables in 8 stations are averaged to be a value that represents the mean daily results of Euphrates water in Al Baghdadi sector. The space dimension becomes spatial reading for the purpose of the time variation approach (Mitas and Mitasova 1999), where one of the purposes of this study is to establish the daily variation of hydrochemical levels and the impact of a rainstorm on the chemical components of the Euphrates river in a short time-space segment. The time series of Euphrates river water chemistry are dominated by fluctuated peaks associated with high-

Table 2 Physico-chemical variables of the Euphrates river water

Variable	Min.	Max.	Mean (M) ± standard deviation (SD)
Base-flow water before rainfall 5/2/2018			
pH	7.7	8.2	7.4 ± 0.17
Temperature (°C)	17	18	17.6 ± 0.33
EC (µS/cm)	770	879	820 ± 30.8
TDS (mg/l)	615	765	690 ± 47.3
TH (mg/l)	339	369	354 ± 9.2
TC (mg/l)	27.2	29.1	28.1 ± 0.6
CO_2 (mg/l)	4.5	4.8	4.6 ± 0.18
K(mg/l)	1.9	4.7	3.3 ± 1.03
Na (mg/l)	55	102	67.2 ± 14.1
Mg (mg/l)	33	42	35.8 ± 2.75
Ca (mg/l)	78	85	81.5 ± 2.33
Cl (mg/l)	100	164	114 ± 19.6
SO_4 (mg/l)	219	256	237 ± 14.1
HCO_3 (mg/l)	120	124	121 ± 2.5
pH	7.75	7.85	7.8 ± 0.03
Temperature (°C)	14	15	14.5 ± 0.34
EC (µS/cm)	775	830	802 ± 16.6
TDS (mg/l)	484	778	605 ± 106.2
TH (mg/l)	244.7	277.8	261 ± 10.7
TC (mg/l)	28.3	33.4	30.8 ± 1.49
CO_2 (mg/l)	4.8	6.5	5.6 ± 0.48
K (mg/l)	1.5	4.7	3.1 ± 1.09
Na (mg/l)	40.7	126.4	73 ± 27.1
Mg (mg/l)	27.8	45	31.7 ± 5.37
Ca (mg/l)	57.4	72.12	62.5 ± 5.0
Cl (mg/l)	84	117	94.7 ± 10.4
SO_4 (mg/l)	140	310	202 ± 57.9
HCO_3 (mg/l)	124.8	171.6	137.7 ± 13.7
Rainwater 16/2/2018			
pH	7.02	7.5	7.26 ± 0.2
Temperature (°C)	12	13	12.5 ± 0.4
EC (µS/cm)	111	200	155 ± 36
TDS (mg/l)	82	140	115 ± 23
TH (mg/l)	11.04	33.12	22.08 ± 9
TC (mg/l)	36.4	50.9	43.6 ± 6
CO_2 (mg/l)	6.4	8.9	7.6 ± 1
K (mg/l)	0.7	2.3	1.5 ± 0.6
Na (mg/l)	13.8	35.4	24.6 ± 9
Mg (mg/l)	1	4	2.5 ± 1.2
Ca (mg/l)	5.8	7.4	6.6 ± 0.6
Cl (mg/l)	9.4	14	11.7 ± 2
SO_4 (mg/l)	40	60	50 ± 8
HCO_3 (mg/l)	15.6	21.4	18.5 ± 2
Euphrates water after rainfall 18/2/2018			
pH	7.3	8.0	7.65 ± 0.22
Temperature (°C)	16	17	16.7 ± 0.33
EC (µS/cm)	810	985	897 ± 50.8
TDS (mg/l)	628	705	666 ± 24.7

Table 2 (continued)

Variable	Min.	Max.	Mean (M) ± standard deviation (SD)
TH (mg/l)	338	350	344 ± 3.78
TC (mg/l)	26.5	30.2	28.3 ± 1.08
CO_2 (mg/l)	4.3	4.9	4.6 ± 0.18
K(mg/l)	2.3	5.5	3.3 ± 0.93
Na (mg/l)	64.3	82.7	73.5 ± 5.88
Mg (mg/l)	30	34	32 ± 1.19
Ca (mg/l)	82	85	83 ± 1.08
Cl (mg/l)	94	108	101 ± 4.73
SO_4 (mg/l)	238	270	254 ± 11.1
HCO_3 (mg/l)	113	129	121 ± 4.63

flow events (during a rain storm), with decreasing values of all parameters due to dilution process before back to the baseline value, as shown in Fig. 4.

The physico-chemical component ranking of Euphrates water during the monitoring periods was achieved using Spearman correlation coefficient (Helsel and Hirsch 2002). Therefore, Spearman's rank correlation coefficients were employed to illustrate and measure associations between variables (Guey-Shin et al. 2011). The Spearman correlation evaluates the monotonic relationship between two continuous or ordinal variables. The Spearman correlation coefficient is based on the ranked values for each variable rather than the raw data. Spearman correlation is often used to evaluate relationships involving ordinal variables. For example, you might use a Spearman correlation to evaluate whether the order in which employees complete a test exercise is related to the number of months they have been employed.

$$r_s = 1 - 6\sum \frac{d_i^2}{n(n^2-1)} \tag{1}$$

where $d_i = x_i - y_i$ represents the difference in ranks for the ith individual and n denotes the number of individuals.

r_s can take values from +1 to −1, where;

- r_s of +1 indicates a perfect association of ranks.
- r_s of zero indicates no association between ranks.
- r_s of −1 indicates a perfect negative association of ranks. The closer r_s to zero, is the weaker.

The daily pattern observed in water chemistry time series indicates significant distortion in the concentration of all parameters with a variable coefficient of > 5% except for water temperature and pH. The variation in concentration contributed to the hydrogeochemical processes (high dilution capacity and mixing-dispersion mechanisms during rainstorm period) and the other natural geochemical cycles within the river. The values of electrical conductivity and TDS for the waters of the Euphrates river fluctuate in a significant level with coefficient of variation, CV% of 30.0 and 36.7 ranged between values of (M + SD) and (M − SD), respectively. Also, the soluble salt contents of the water affected the conductivity value. The salt content slightly increases with waste disposal site age as a consequence of the decomposition of organic matter (Nakhaei et al. 2015).

Accordingly, the Euphrates river in Al Baghdadi sector can be considered as zone of natural water without pollution hotbeds. On the other hand, a statistical comparison of hydrochemical variables against river discharge is computed as Spearman correlation coefficient values (Table 4).

The negative associations of ranks are noticed between river discharge and all parameters during high flow except for pH, TC, CO_2, and HCO_3^-, which have a positive association of ranks. The results indicate the impact of storm event on the quality of water (high dilution capacity) with high influence of rain, CO_2 contents, which caused high bicarbonate and total carbon concentrations then raised pH values.

Figure 5 shows the variation of physico-chemical parameters during different periods (before, during, and after storm event), which reflects the phenomenon of water dilution and mixing. The rate of mixing of the Euphrates water in Al-Baghdadi sector during rainstorm was calculated using chloride ion concentration as shown in the following equation. The concentration of chloride is used in the calculation of mixing ratio ($R\%$) because it is less affected by chemical reactions in aqueous environment (Langmuir 1997; Mullaney et al. 2009).

$$R\% = \left\{\left[Cl^-_{\text{base-flow}}\right] - \left[Cl^-_{\text{high-flow}}\right]\right\} / \left\{\left[Cl^-_{base-flow}\right] - \left[Cl^-_{\text{rain water}}\right]\right\} \times 100 \tag{2}$$

where $R\%$: proportion of Cl^- concentration in rainwater mixing with a Cl^- concentration in river water.

$Cl^-_{\text{base flow}}$: chloride concentration (mean value) of Euphrates water before rainstorm, (Table 2).

$Cl^-_{\text{high flow}}$: chloride concentration (mean value) of Euphrates water during rain storm.

$Cl^-_{\text{rain water}}$: chloride concentration (mean value) of rain water.

$R\%$ = {(114 mg/L−94.7 mg/L)/(114 mg/L−11.7 mg/L)} × 100 = 18.8%

This means 81.2% of Cl^- in Euphrates water (during a rainstorm) derived from river base flow (before rainstorm) and 18.8% comes from rainstorm. The mixing percents represent a case of multi-source water happened as a result of dilution, caused by direct rainfall on river sector. The abovementioned results calculated under following facts condition:

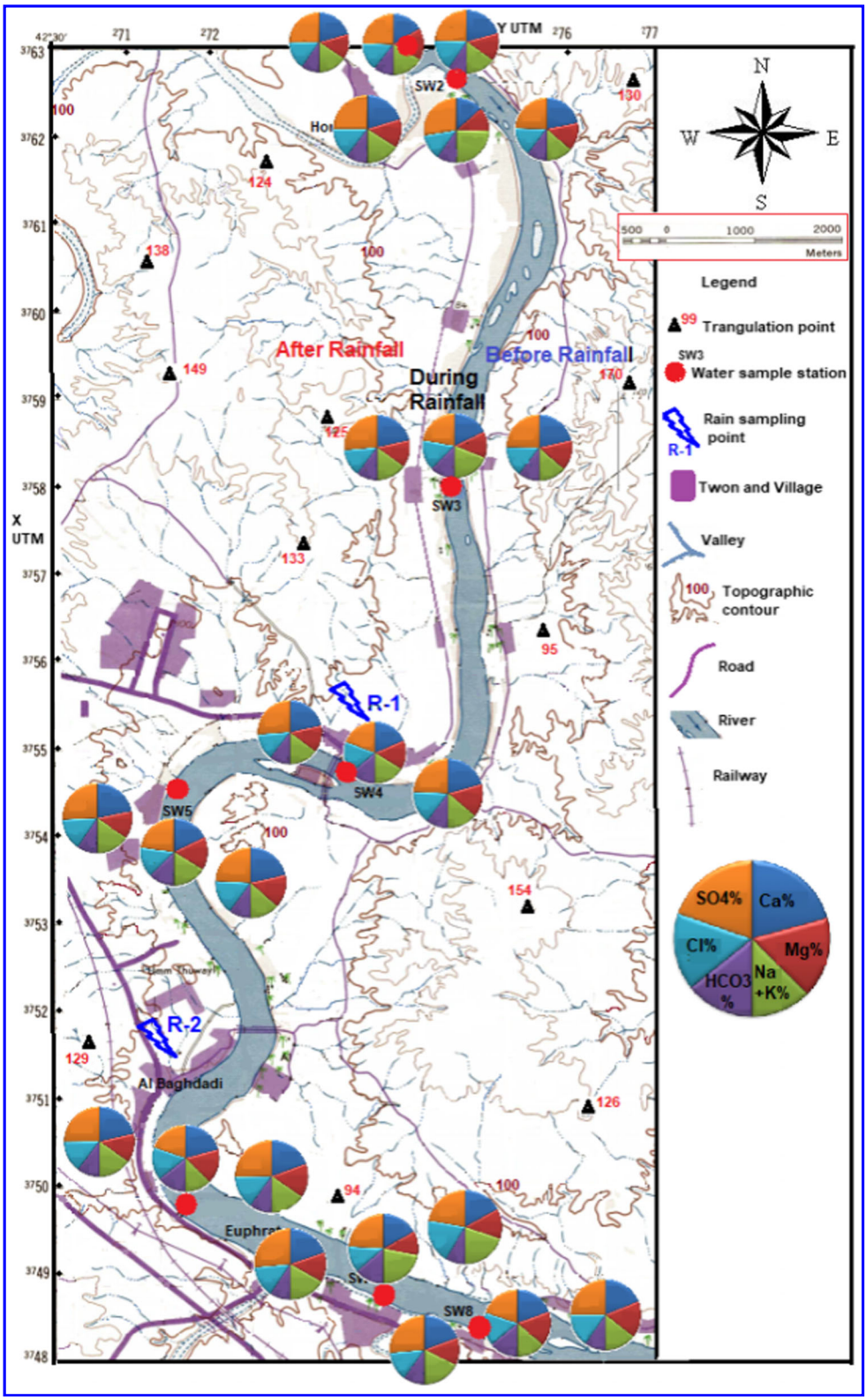

Fig. 3 Spatial distribution map of Euphrates major ions within Al Baghdadi sector

1- The amount of rainwater that fell on the Euphrates river sector during rainstorm (16/2/2018) was 0.112×10^6 m^3/day, with a total dissolved load of 12.88 tons/day (115 mg/L × 0.112×10^6 m^3/day × 10^{-6}) added to the river.

2- The river discharge in the day of storm event during high-flow period was 21.92×10^6 m^3/day, with a total dissolved load discharge of 13,261 tons/day (605 mg/L × 21.92×10^6 m^3/day × 10^{-6}) passes through river sector.

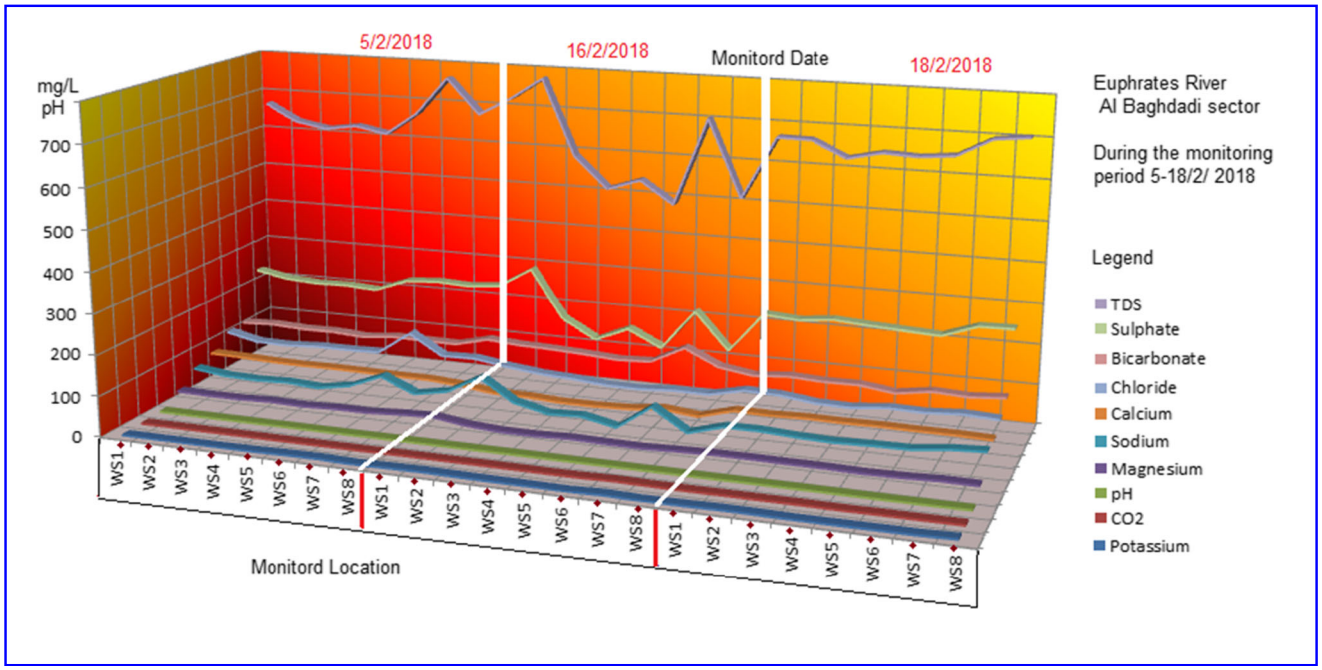

Fig. 4 Water quality space-time series of Euphrates river

3- The river discharge before storm event during base-flow period was 21.6×10^6 m^3/day, with a dissolved load discharge of 14,904 tons/day (690 mg/L × 21.6×10^6 m^3/day × 10^{-6}) passes through river sector.

Comparisons were made using a number of standard statistical techniques. The statistical results for each component, including mean (M) , M+SD, M−SD, standard deviation (SD) and coefficient of variation (CV%), and Spearman correlation coefficient (r_s), are used in the interpretation and limiting each

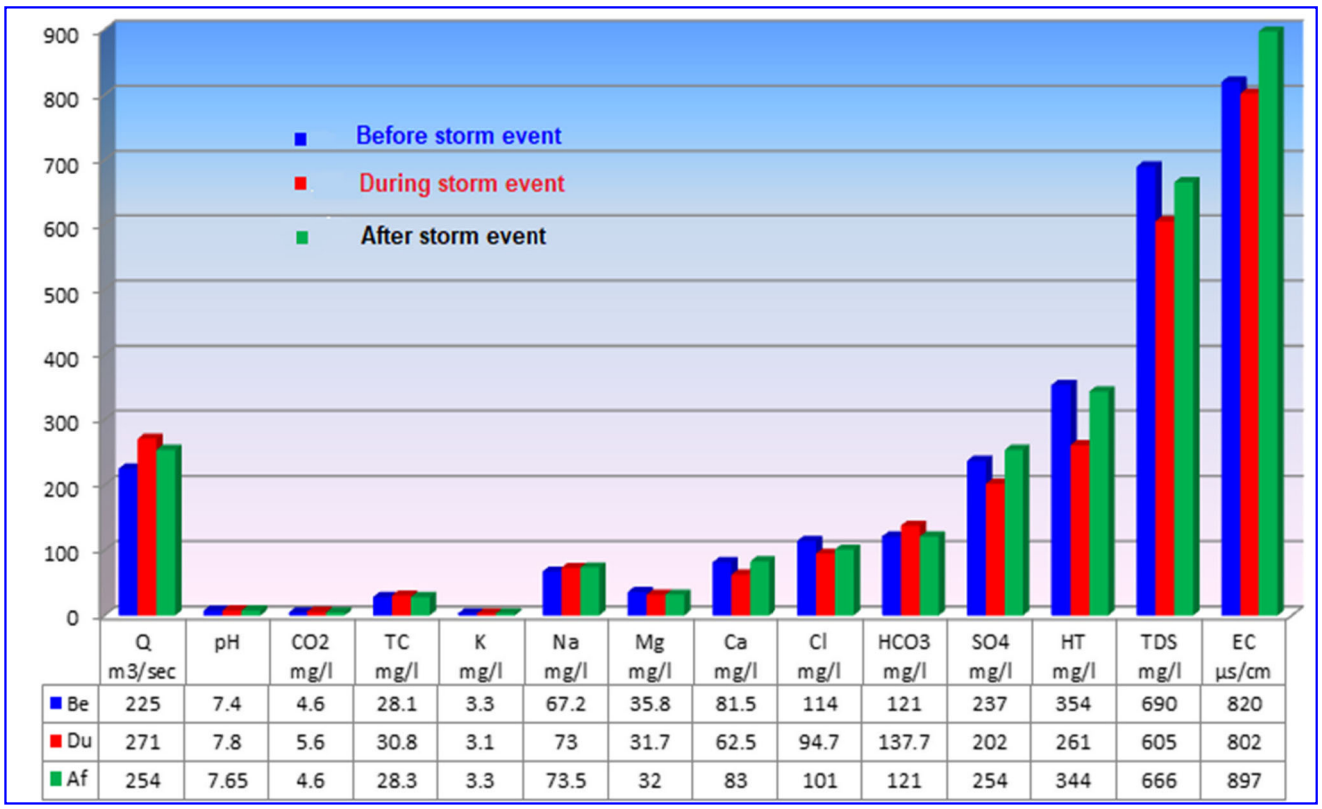

	Q m3/sec	pH	CO2 mg/l	TC mg/l	K mg/l	Na mg/l	Mg mg/l	Ca mg/l	Cl mg/l	HCO3 mg/l	SO4 mg/l	HT mg/l	TDS mg/l	EC µs/cm
Be	225	7.4	4.6	28.1	3.3	67.2	35.8	81.5	114	121	237	354	690	820
Du	271	7.8	5.6	30.8	3.1	73	31.7	62.5	94.7	137.7	202	261	605	802
Af	254	7.65	4.6	28.3	3.3	73.5	32	83	101	121	254	344	666	897

Fig. 5 Physico-chemical parameters of Euphrates river before, during, and after rainstorm

variable fluctuation in space and time dimension (Helsel and Hirsch 2002).

Saturation index is expressed as: SI = log (IAP/Ksp) where IAP is the ion activity product and Ksp is the solubility product of the mineral. The saturation index values of soluble minerals in water samples are calculated by the PHREEQC software (Parkhurst and Appelo 1999). The concentrations of the chemical constituents of the waters are correlated with the various quality criteria to identify the probability of use. Quality criteria of water for domestic and drinking uses have been proposed by various national and international agencies such as the World Health Organization (WHO 2011) and US Environmental Protection Agency (USEPA 2002), as revealed in Table 3.

Sodium adsorption ratio is an estimate of the extent to which sodium ion present in the water would be adsorbed by the soil and is expressed by the equation (Amiri et al. 2015)

$$\mathrm{SAR} = \mathrm{Na}/[(\mathrm{Ca}+\mathrm{Mg})/2]^{1/2} \quad (3)$$

where SAR criteria against salinity in USSLS diagram is used for irrigation application (agriculture purpose) (USSLS 1954), sodium, calcium, and magnesium are in meq/l. River water samples were evaluated for animal drinking water purpose using US. The Public Health Service classification is shown in Table 4.

The quality requirements for industrial water supplies are widely extended, and water of TDS values less than 500 mg/L which is admissible for many industrial uses. The varied nature of the requirements for some industries can be obtained from data presented by the U.S. Federal Water Pollution Control Administration (Walton 1970).

Table 4 Water quality standards for human drinking and livestock watering

Constituents	Human drinking		Animal watering
	WHO 2011	USEPA 2002	TDS mg/L
pH	7-8.5	6.5-8.5	0-1000
TDS (mg/L)	500	500	
K^+ (ppm)	-	-	1000-3000
Na^+ (ppm)	200	-	
Ca^{+2} (ppm)	75	-	3000-5000
Mg^{+2} (ppm)	30	-	
HCO_3^- (ppm)	200	-	5000-7000
Cl^- (ppm)	250	250	
SO_4^{-2} (ppm)	200	250	7000-13,000
NO_3^- (ppm)	50	44	
H_T (ppm)	500	-	

Canadian Council of Ministers of the Environment (CCME) has developed Water Quality Index (WQI) which is a one of the major tool to solve the problems of data management and to evaluate success and failures in management strategies for improving water quality. Three measures were selected to calculate the CWQI (F_1= scope, F_2 = frequency and F_3= amplitude) as follows: (CCME, 2001).

$$F_1 = (\text{Number of failed variables}/\text{Total number of variables}) \times 100$$

$$F_2 = (\text{Number of failed tests}/\text{Total number of variables}) \times 100$$

$$\text{Excursion}_i = \left(\text{failed test value}_i/\text{objective}_j\right) - 1$$

Table 3 Statistical results of the physico-chemical variables of the Euphrates water (5-18/2/2018)

Variable	Min.	Max.	Mean (M) ± standard deviation (SD)	Cv %	Spearman rank coefficient r_s
Q (m^3/s)	250	254	252 ± 2	0.8	1.0
pH	7.3	8.2	7.5 ± 0.2	2.6	0.287
Temperature (°C)	14	18	16 ± 0.33	2.0	−0.612
EC (μS/cm)	770	985	842 ± 53.7	6.4	−0.012
TDS (mg/l)	484	778	609 ± 158	25.9	−0.162
HT (mg/L)	244	369	318 ± 39.7	12.5	−0.612
TC (mg/L)	26.5	33.4	29.4 ± 1.54	5.2	0.587
CO_2 (mg/L)	4.3	6.5	4.65 ± 0.4	8.6	0.675
K^+ (mg/L)	1.5	4.7	2.88 ± 1.1	38.2	−0.075
Na^+ (mg/L)	40.7	126.4	68.6 ± 23.8	34.7	0.137
Mg^{+2} (mg/L)	27.8	45	31.9 ± 8.5	26.6	−0.162
Ca^{+2} (mg/L)	57.4	85	70.5 ± 9.8	13.9	−0.612
Cl^- (mg/L)	84	164	99.8 ± 28.2	28.2	−0.312
SO_4^{-2} (mg/L)	140	310	217 ± 63	29.0	−0.162
HCO_3^- (mg/L)	113	171.6	121 ± 31.8	26.3	0.737

$$\text{Excursion}_i = \left(\text{objective}_j/\text{failed test value}_i\right)-1$$

$$\text{nse} = (\Sigma_1{}^n \text{ excursion}_i)/\text{number of tests}$$

$$F_3 = \text{nse}/\{0.01\ \text{nse} + 0.01\}$$

CCME WQI

$$= 100-\left[\sqrt{\left\{(F_1)^2 + (F_2)^2 + (F_3)^2\right\}}/1.732\right] \quad (4)$$

Annual chemical components export in the river Euphrates was calculated using a standard flux-based algorithm based on metrics of instantaneous discharge and concentration (Walling and Webb 1985; Littlewood and Marsh 2005; Johnes 2007).

Load discharge (ton/day) = Water discharge (Q) (m^3/day) × Concentration (C) (mg/L) × 10^{-6}.

Hydrochemical facies and classification

The chemical character of the Euphrates water within the second hydro-meteorological subsystem has been determined by the application of hydrochemical facies, which reflects the effect of chemical processes (exposed rocks-surface water interactions). The concept of hydrochemical facies was developed in order to understand and identify the water composition in different classes (Masoumi et al. 2016).

The ion dominance order reflects the weathering degree within a hydrologic system and watershed areas. Euphrates water facies in the study region during the monitoring period reveals the majority percent of sulfate group (100%), classified as Ca and Na-sulfate families in a percent to 79% and 21%, respectively.

All such sulfate types are the result of hydrochemical processes acting between water and rock matrix such as leaching and the dissolution of evaporite and carbonate rocks, while the variation reflects the effectiveness of the water flow path (Appelo and Postma 2005). The water-rock interaction can alter water with high $SO_4{}^{-2}$ concentrations associated with the dissolution of gypsum, which is commonly encountered within exposure media.

The statistical distribution diagram (Piper Trilinear in Fitts 2002) was applicated for the purpose of characterizing river water types. The plotted points of river water analyses in the Fig. 6 explained the majority of Ca^{+2} and Mg^{+2} than Na^+ and K^+ cations. Also, the dominance of $SO_4{}^{-2}$ and Cl^- anions than $CO_3{}^{-2}$ and $HCO_3{}^-$, which hold the water to be about non-carbonate hardness behavior, classifying it as Ca–Mg; Cl-sulfate water type, representing the condition of moderate active hydrologic system (Amiri et al. 2016).

Hydrochemical evolution of water

The presentation of water chemistry on the expanded Durov diagram (Chadha 1999) is used to determine the hydrogeochemical evolution trend of the water within hydrologic system. The results of plotting chemical data on expanded Durov's diagram are used to identify the evolution of water where the water is initially recharged by Ca-HCO_3 water (rain water) and undergoes water-rock interactions (dissolution) then mixing with pre-existing water along the flow path (Hussien and Faiyad 2016). This leads to the evolution of Ca-SO_4, Mg-SO_4, and Na_2SO_4 water types and finally reaches an advanced state of geochemical evolution, which is represented by the Na-Cl type.

Figure 7 explains that the Euphrates water collected from eight locations is mainly plotted in field no. 5 symbolized by a Ca-Mg; Cl-sulfate water types, denoting mixed water type, influenced by dissolution mechanism, and is possibly developed from Ca-HCO_3 recharge water, influenced by ion exchange mechanism. Also, limited reverse ion exchange process has been noticed in some water samples.

Impact of hydrochemistry on the evolution of Euphrates water

The saturation index (SI) and solution–mineral equilibria (mineral balance) calculations are used to predict the interaction of minerals within the hydrological system. The negative index (SI < 0) refers to under saturation conditions. A positive indicator (SI > 0) denotes that water is over-saturated with respect to a particular mineral phase, while neutral SI (SI = 0) explains the equilibrium state with the specified mineral phase (Stumm and Morgan 1981).

The calculated saturation index values of the eight minerals (Table 5) demonstrate that all water samples are undersaturation with respect to dolomite, calcite/aragonite, gypsum/anhydrite, and halite/sylvite.

The various negative values of SI indicate the occurrence of chloride, carbonate, sulfate dissolution from their mineral phases within Euphrates riverbed and its catchment area. This phenomenon leads us to deduce that the evolution of sulfate water types is nearly reaching the neutral SI state of evolution, which reflects the state of the river transitional zone with local, replenish charge zones (Haditha lake).

The second factor that affect on the hydrochemistry of Euphrates water is the evaporation process which causes increased in concentrations of water components. Na/Cl ratio is good indicative factors used in distinguishing the effectiveness of the evaporation process on water chemistry. The very high correlation between Na and Cl (about 1.3) may indicate the equal influx of these ions into groundwater through halite dissolution (Amiri et al. 2020).

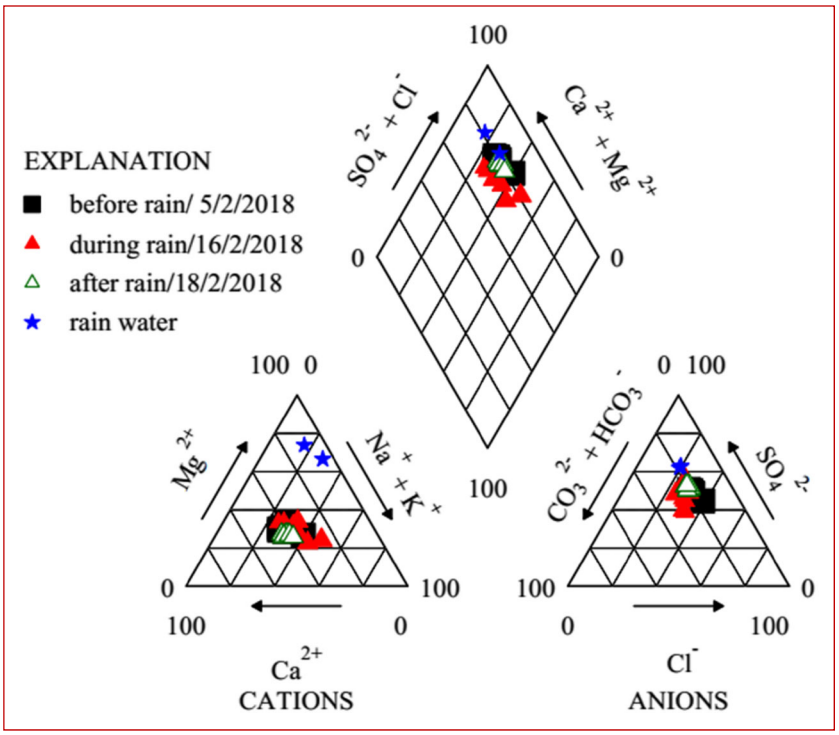

Fig. 6 Water quality of Euphrates samples plotted on Piper diagram

Chloro-alkaline index (CAI) = $[Cl^- - (Na^+ + K^+)]/Cl^-$; saturation index (SI) = log (IAP/Ksp), Ksp = solubility product constant, ion activity product (IAP).

Almost Na/Cl ratio remains steady in case of water evaporation which causes high TDS concentration in surface water (Jankowski and Acworth 1997), also Sami (1992)

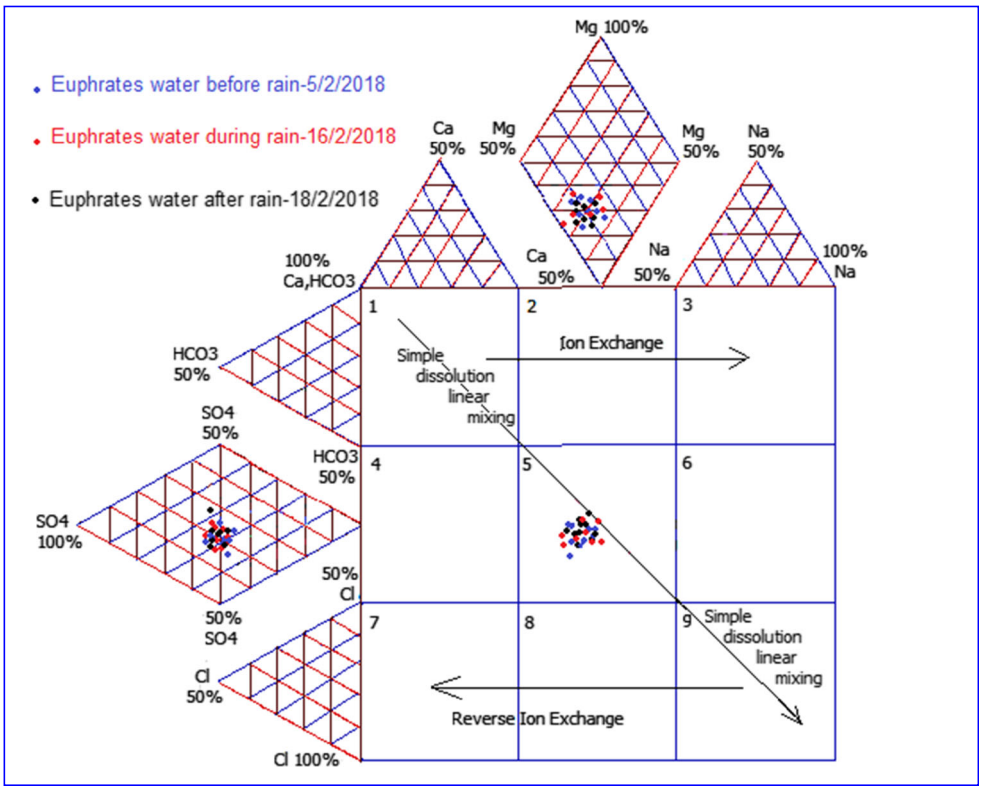

Fig. 7 Plotting of water analyses on expanded Durov diagram

Table 5 Saturation and hydrochemical indices of the Euphrates and rain water

Date sampling	St. no.	SI Calcite	SI Aragonite	SI Dolomite	SI Gypsum	SI Anhydrite	SI Halite	SI Sylvite	CO_2I	Na^+/Cl^-	CAI= $Cl^- - (Na^+ + K^+)/Cl^-$
5/2/2018	WS1	−0.56	−0.70	−1.17	−1.26	−1.56	−6.68	−7.71	−1.96	0.91	0.08
	WS2	−0.54	−0.69	−1.15	−1.28	−-1.59	−6.81	−7.85	−1.94	0.93	0.08
	WS3	−0.57	−0.72	−1.19	−1.30	−1.60	−6.83	−7.86	−1.95	0.9	0.09
	WS4	−0.58	−0.72	−1.16	−1.31	−1.61	−6.79	−7.84	−1.95	0.9	0.1
	WS5	−0.58	−0.73	−1.20	−1.31	−1.61	−6.82	−7.69	−1.97	0.9	0.16
	WS6	−0.58	−0.72	−1.15	−1.27	−1.58	−6.72	−7.49	−1.94	1.0	−0.03
	WS7	−0.59	−0.74	−1.18	−1.28	−1.59	−6.37	−7.27	−1.95	1.0	0.01
	WS8	−0.59	−0.73	−1.11	−1.28	−1.59	−6.71	−7.72	−1.95	0.93	0.08
	Minimum	−0.54	−0.69	−1.11	−1.26	−1.56	−6.37	−7.27	−1.94	0.9	−0.03
	Maximum	−0.59	−0.74	−1.20	−1.31	−1.61	−6.83	−7.86	−1.97	1.0	0.16
	Mean	−0.57	−0.72	−1.16	1.28	−1.59	−6.6	−7.56	−1.95	0.94	0.07
16/2/2018 During rainstorm	WS1	−0.56	−0.71	−1.00	−1.31	−1.62	−6.61	−7.49	−1.88	1.1	−0.11
	WS2	−0.66	−0.81	−1.26	−1.30	−-1.61	−6.47	−7.46	−1.90	1.9	−0.94
	WS3	−0.62	−0.76	−1.25	−1.45	−1.75	−6.73	−7.62	−1.90	1.2	−0.22
	WS4	−0.64	−0.79	−1.26	−1.58	−1.88	−6.87	−7.74	−1.91	0.95	0.05
	WS5	−0.68	−0.82	−1.28	−1.50	−1.80	−6.89	−7.84	−1.93	1.1	−0.09
	WS6	−0.63	−0.77	−1.23	−1.57	−1.87	−7.04	−8.02	−1.92	0.8	0.23
	WS7	−0.49	−0.63	−1.04	−1.33	−1.64	−6.63	−7.56	−1.80	1.8	−0.75
	WS8	−0.62	−0.76	−1.19	−1.55	−1.85	−6.95	−7.90	−1.91	0.84	0.16
	Minimum	−0.49	−0.63	−1.00	−1.30	−1.61	−6.47	−7.46	−1.80	0.8	−0.94
	Maximum	−0.68	−0.82	−1.28	−1.58	−1.88	−7.04	−8.02	−1.93	1.9	0.23
	Mean	−0.59	−0.72	−1.19	−1.44	−1.75	−6.75	−7.74	−1.87	1.3	−0.21
18/2/2018	WS1	−0.56	−0.71	−1.20	−1.25	−1.55	−6.70	−7.68	−1.96	1.04	−0.04
	WS2	−0.55	−0.69	−1.15	−1.27	−1.57	−6.71	−7.54	−1.93	1.1	−0.08
	WS3	−0.54	−0.69	−1.18	−1.24	−1.54	−6.78	−7.62	−1.94	1.1	−0.11
	WS4	−0.55	−0.69	−1.17	−1.25	−1.55	−6.81	−7.81	−1.94	1.08	−0.08
	WS5	−0.58	−0.72	−1.28	−1.25	−1.55	−6.75	−7.70	−1.98	1.03	−0.09
	WS6	−0.54	−0.68	−1.17	−1.26	−1.56	−6.75	−7.65	−1.93	1.07	−0.07
	WS7	−0.56	−0.71	−1.18	−1.23	−1.53	−6.67	−7.63	−1.95	1.15	−0.15
	WS8	−0.55	−0.69	−1.16	−1.23	−1.53	−6.66	−7.40	−1.92	1.3	−0.28
	Minimum	−0.54	−0.68	−1.15	−1.23	−1.53	−6.66	−7.40	−1.92	1.03	−0.04
	Maximum	−0.58	−0.72	−1.28	−1.27	−1.57	−6.81	−7.81	−1.98	1.3	−0.28
	Mean	−0.56	−0.70	−1.21	−1.25	−1.55	−6.78	−7.65	−1.95	1.16	−0.11

recommends to use Na/Cl ratio in determining the mechanism of salinity distribution (Sami 1992).

The relation between TDS and Na/Cl ratio of the Euphrates water samples (Fig. 8) illustrates positive trend line controlled by a 3rd relation fit of:

$$\mathrm{Na/Cl} = -6.385 + 0.0343(\mathrm{TDS}) + 5\mathrm{E}{-}05(\mathrm{TDS})^2 + 3\mathrm{E}{-}08(\mathrm{TDS})^3 \quad (5)$$

The Na/Cl ratio only remains stable with the increasing salinity in the sector of TDS ranging between 600 mg/L and 723 mg/L, indicating the effectiveness of evaporation on the water samples of the Euphrates river before and after a rain shower with the exception of Euphrates water during rain period.

The Na/Cl values (Table 5) are greater than its value in seawater (0.87), which indicates partial leaching of continental sediments with hosted sodium content. The low potassium concentration in Euphrates river is due to its tendency to be stabilized according to the process of cation exchange between clay minerals, secondary salts with its accompanying

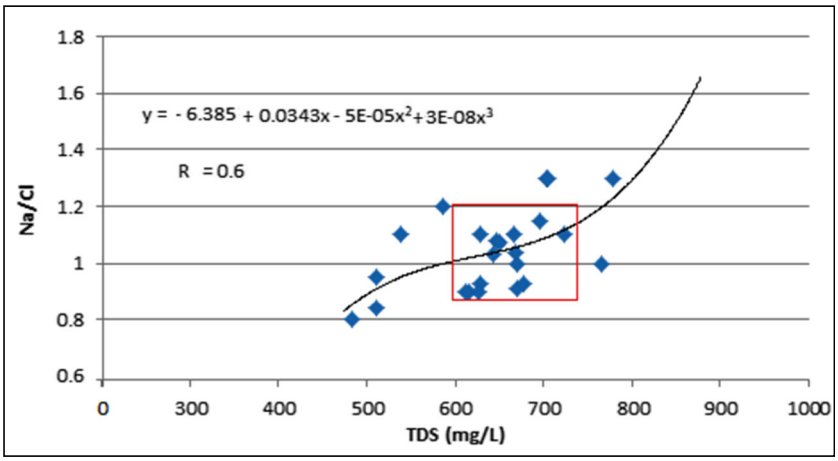

Fig. 8 TDS v's Na/Cl scatter diagram

water (Zhu et al. 2008; Matthess 1982). Also, Appelo and Postma (2005) describe the cation exchange as a factor modifying water quality and a process related to water-rock interaction. The chloro-alkaline index as explained by Schoeller equation (Schoeller 1977);

$$CAI = [Cl - (Na + K)]/Cl \quad (6)$$

where used to categorize and separate between normal and reverse ion exchange process. Accordingly, the results of the chloro-alkaline index of the water samples within the study area (Table 5) indicate the following:

- A normal ion exchange process happened in the period before rainfall (an exchange between Na and/or K (water) with Ca and/ or Mg (in riverbed material)), where the results of CAI index are negative.
- A reverse ion exchange with positive index was happened during and after rain period (Ca and/or Mg (water) replaced by Na and/or K (in riverbed material)). The exchange is known as direct when the indices are positive. If the exchange is reversed, then the exchange is indirect and the indices are found to be negative. The results indicated that the ion exchange can be controlled by rock/water interactions, dissolution of evaporation deposits, and precipitation-dissolution of carbonates (Amiri et al. 2015).

Assessment of water quality for various purposes and uses

Potability of water for drinking and domestic uses

The analytical results of the Euphrates water samples have been compared with the standard guideline values suggested by the World Health Organization (WHO 2011). The comparison results are concluded in the following:

- The pH of the groundwater samples is safe limit of 6.5-8.5 (Sohrabi et al. 2017).
- The total dissolved solid exceeded the desirable limit (500 mg/L), classified as fair water in water samples before and after rainfall except for samples collected during rainfall, which were classified as good water.
- The total hardness values of the water samples during the monitoring period are desirable limit of 300 mg/L and less than the maximum permissible limit (500 mg/L), then categorized as hard to very hard water (Todd and Mays 2005).
- The SO_4 concentrations existed in the marginal class within the maximum permissible limit (200-250 mg/L) in all water samples.
- The HCO_3 and Cl concentrations of water samples are not exceed the recommended limit of both 200 and 250 mg/L, respectively.
- The magnesium and calcium concentrations exceed the maximum admissible limit 30 and 75 mg/L in the water samples that collected before and after a rainstorm while their concentrations are permissible limit during rain period, where Na concentrations less than the recommended level (200 mg/L) in all water samples.

The concentrations of Euphrates water salinity are compared with the Water Quality Standards for Livestock Use recommended by Crist and Lowry (1972). The comparison results categorized Euphrates water as good class within the safe limits for animals drinking, e.g., poultry, camels, sheep, horses, dairy, and beef cattle according to specific classification in Lewen and King (1971).

Potability of Euphrates water for industrial uses

The quality criteria of water for industrial purposes depend on the type of industry, processes, and products (McKee and Wolf 1963). Low pressure boilers can be used water with total dissolved solids up to 700 mg/L and $CaCO_3$ hardness up to 20

mg/L; therefore, the Euphrates water can be used in this employ, while in high pressure boilers total dissolved should be less than 50 mg/L and hardness < 1 mg/L (Hem 1989), accordingly the Euphrates water is not recommended for this use.

Comparing of sulfate content in water samples with the maximum permissible limit of SO_4 (1500 ppm) proceeded by Altoviski (1962), indicates the suitability of Euphrates water for use in construction industries. The corrosivity ratio values as calculated by relation (Golekar et al. 2014);

$$CR = (Cl + SO_4)/\{2(HCO_3 + CO_3)\} \quad (7)$$

where ranged between 1.25 and 3.66 in the Euphrates water within the study region (Table 6). Corrosivity ratio indicates that Euphrates water is unsafe (CR > 1) against metallic materials.

Suitability of Euphrates water for irrigation purposes

The earliest systems of quality water standards for irrigation use were given by USSLS (1954). The total salinity concentration, residual sodium carbonate (RSC), sodium adsorption ratio (SAR), and Kelley index (KI) are the remarkable indices used for appraising the suitability of water for irrigation purposes (Ayers and Westcot 1985). The result of residual sodium carbonate (RSC) is calculated from following equation (Karanth 1989);

$$(RSC) = \left(CO_3^- + HCO_3^-\right) - \left(Ca^{+2} + Mg^{+2}\right) \quad (8)$$

All collected water samples are less than (1.5 meq/L) and in negative content (Table 7). This means there is no excess of sodium carbonate in Euphrates water, which reflects the suitability of water for irrigation purposes as confirmed by Kelley's index [$Na^+/(Ca^{+2} + Mg^{+2})$] (Kelley 1946; Paliwal 1967) results, which varied between 0.33 and 0.93 (KI < 1, refer to suitable for irrigation).

Also, output plot data detected from Rechards diagram (USSLS 1954) (Fig. 9), in which the EC is taken as salinity hazard and SAR as alkalinity hazard [$Na^+/(\sqrt{(Ca^{+2} + Mg^{+2})/2}$]

Table 7 Hydrochemical indices for the water uses within study region

Date sampling	Station no.	Corros. ratio	SAR	RSC	KI
5/2/2018	WS1	2.13	1.58	−5.2	0.42
	WS2	1.86	1.37	−4.87	0.37
	WS3	1.89	1.36	−4.79	0.37
	WS4	1.92	1.39	−4.97	0.37
	WS5	1.97	1.3	−4.93	0.35
	WS6	2.02	1.6	−5.0	0.42
	WS7	2.47	2.38	−4.97	0.63
	WS8	2.12	1.5	−5.4	0.39
Minimum		1.86	1.3	−4.79	0.35
Maximum		2.47	2.38	−5.4	0.63
Mean		2.14	1.56	−5.1	0.41
16/2/2018 During rain shower	WS1	1.87	1.86	−5.02	0.49
	WS2	1.45	3.2	−3.65	0.93
	WS3	1.51	1.94	−3.22	0.59
	WS4	1.31	1.5	−3.04	0.46
	WS5	1.5	1.53	−3.41	0.47
	WS6	1.25	1.1	−3.32	0.33
	WS7	1.34	2.55	−2.98	0.75
	WS8	1.3	1.23	−3.42	0.37
Minimum		1.25	1.1	−2.98	0.33
Maximum		1.87	3.2	−5.02	0.93
Mean		1.45	1.86	3.51	0.68
18/2/2018	WS1	2.09	1.66	−4.99	0.44
	WS2	1.93	1.68	−4.77	0.45
	WS3	1.96	1.56	−4.89	0.42
	WS4	1.91	1.51	−4.79	0.41
	WS5	2.14	1.58	−4.9	0.43
	WS6	1.89	1.6	−4.72	0.44
	WS7	2.15	1.81	−5.03	0.48
	WS8	2.02	1.94	−4.74	0.52
Minimum		1.89	1.51	−4.72	0.41
Maximum		2.15	1.94	−5.03	0.52
Mean		2.02	1.72	−4.88	0.44

Corrosion ratio (CR) = $(Cl^- + SO_4^{-2})/2(HCO_3^- + CO_3^-$; Kelley index (KI) = $Na^+/(Ca^{+2} + Mg^{+2})$; residual sodium carbonate (RSC) = $(CO_3^- + HCO_3^-) - (Ca^{+2} + Mg^{+2})$; sodium adsorption ratio (SAR) = $Na^+/(\sqrt{(Ca^{+2} + Mg^{+2})/2})$

Table 6 Comparison of few studies in the above section in terms of water quality parameters

pH groundwater	TDS (mg/L)	Hardness (mg/L)	SO_4 concentrations (mg/L)	HCO_3 and Cl concentrations (mg/L)	References
6.5-8.5	3669	300	200	250	Rana et al. (2018)
5.5-9.2	2100	740	600	800	Sharma et al. (2020)
6.5-8.5	500	200	400	250	Vasistha and Ganguly 2020a, 2020b)
6.5-8.5	500	300-500	200-250	200-250	This work

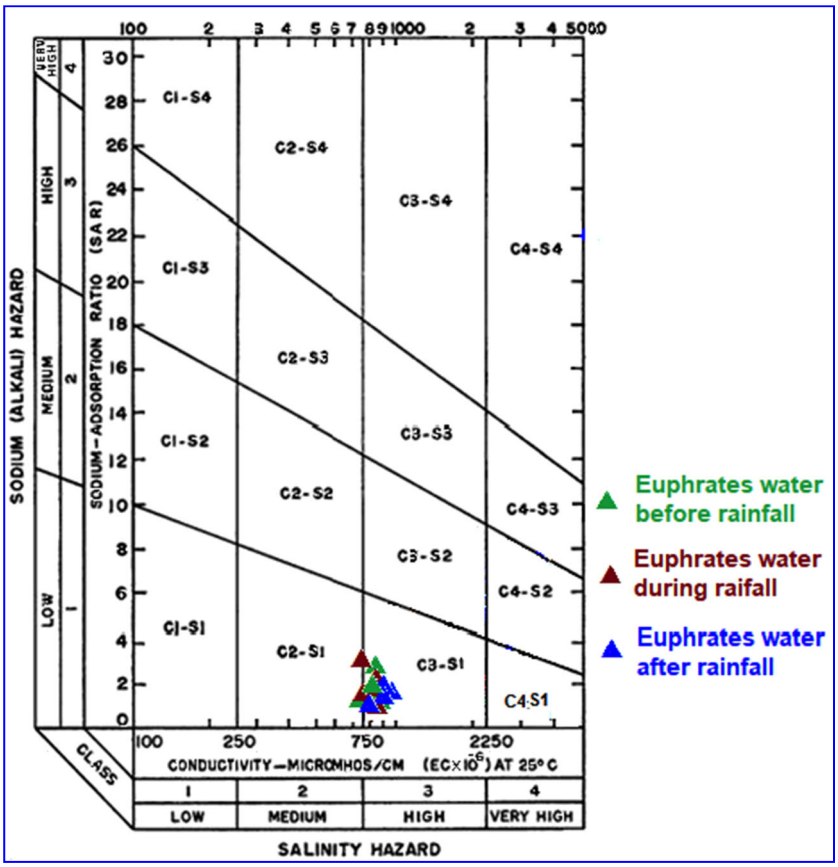

Fig. 9 Plot SAR and ECx10^{-6} data on (USSLS 1954) diagram

shows that all water samples are categorized within C3S1 and C2S1 denoting:

- Good quality for irrigation with little danger of harmful levels against crops and other plants.
- Admissible quality water for irrigation and be used to irrigate salt tolerant and semi-tolerant crops under suitable drainage conditions.

Application of CCME WQI and health of ecosystems (aquatic environment)

The water quality index for the eight stations along the river was determined before, after, and during rainstorms (16/2/2018) using the physicochemical parameters. CWQI of 24 point scale was used to summarize results from different twelve physicochemical measurements. The used parameters are as follows: pH, TDS, H_T, TC, CO_2, K^+, Na^+, Mg^{+2}, Ca^{+2}, Cl^-, SO_4^{-2}, and HCO_3^-. This index reduces huge amounts of data to a single number, thus ranking water into one of five categories, these are the following: very bad water (0-44), bad (45-59), medium (60-79), good (80-94), and excellent quality of the sampled water (95-100) (CCME 2001).

The values of the various scopes (F_1), frequencies (F_2), and amplitudes (F_3), with their respective water quality index in all eight river stations are listed below:

$$F_1 = (\text{Number of failed variables}/\text{Total number of variables}) \times 100$$

$$F_1 = (2/12) \times 100 = 16.66$$

$$F_2 = (\text{Number of failed tests}/\text{Total number of variables}) \times 100$$

$$F_2 = (36/288) \times 100 = 12.5$$

$$\Sigma_1^{\,n}\,\text{Excursion}_i = \left(\text{failed test value}_i/\text{objective}_j\right) - 1 = 4.41$$

$$\text{nse} = (\Sigma_1^{\,n}\,\text{excursion}_i)/\text{number of tests}$$

$$\text{nse} = (4.41)/288 = 0.015$$

$$F_3 = \text{nse}/\{0.01\,\text{nse} + 0.01\}$$

$$F_3 = [0.015/\{0.01\,(0.015) + 0.01\}] = 1.477$$

$$\text{CCME WQI} = 100 - \left[\sqrt{\left\{(F_1)^2 + (F_2)^2 + (F_3)^2\right\}}/1.732\right]$$

$$\text{CCME WQI} = 100 - \left[\sqrt{\left\{(16.66)^2 + (12.5)^2 + (1.477)^2\right\}}/1.732\right]$$

$$= 87.94$$

Accordingly, the water quality of the Euphrates river is rated as good water for aquatic life (healthy ecosystem).

The study encountered some difficulties and obstacles in the sampling sites during the rainstorm, as samples were collected and kept for a long period of time until we got an opportunity to carry out the required tests. We needed to recollect new samples in order to send them to testing centers.

Conclusions

- The hydrochemical facies of river water indicated a hydrologic phenomenon of heterogeneity in the concentrations of major ions, which confirms the role of irregular process of chemical balance resulting from the propagation of mixing, ion exchange, and water-rock interaction between rivers and rainstorm water during high flow period. The results of the chloro-alkaline index (CAI) for the water samples indicate normal ion exchange process happened in the period before rainfall (an exchange between Na^+ and/or K^+ (water) with Ca^{+2} and/ or Mg^{+2} (river basin material), where the results of (CAI) are negative, while reverse ion exchange with positive index happened during and after rain period (Ca^{+2} and/ or Mg^{+2} (water) replaced by Na^+ and/or K^+ (river basin material)). Also, the variation in ion concentration with the flow direction reflects the effectiveness of the flow path, which is commonly encountered ion source within river beds and exposure media. Furthermore, daily records system is recommended for the other sites to complete the regime observation of Euphrates water type.
- The Na^+/Cl^- ratio only remains stable with the increasing salinity in the sector of TDS ranging between 600 and 723 mg/l, indicating the effectiveness of evaporation on the water samples of the Euphrates river before and after a rainstorm, with the exception of Euphrates water during rain period, which dilute the component concentration of river water.
- According to the Piper Trilinear plot, the Euphrates water was categorized as water of non-carbonate hardness represented by Ca^{+2}–Mg^{+2}; Cl^-–SO_4^{-2} water type, occurs in a slightly active zone hydrologic system, this result matched expanded Doruv classification result, where all water analyses plotted in Mg^{+2}–SO_4^{-2} field represented by a Ca^{+2}–Mg^{+2}; Cl^-–SO_4^{-2} water types, indicating mixed water type. The pollution from these sources may have negative effects on the freshwater ecosystem. Treatment units must be installed in each city located on the banks of Euphrates river to mitigate the effectiveness of sewage water and prevents river from pollution.
- The daily pattern observed in water chemistry time series indicates significant distortion in the concentration of all parameters, with a variation coefficient of > 5%. The variation in concentration contributed to dilution capacity and mixing-dispersion mechanisms during rainstorm period. The negative associations of ranks are noticed between river discharge and all parameters during high flow except for pH, TC, CO_2, and HCO_3^-, which have a positive association of ranks. This associations can be removed by filtering process in treatment units.
- The impact of the rainstorm on the quality of water indicates slight dilution capacity with high influence of rain, CO_2 contents, which caused high bicarbonate and total carbon concentrations. The mixing rate (*R*%) referred to chloride concentration caused by direct rainfall on river sector are 81.2% of Cl^- in Euphrates water during rainstorm derived from river baseflow before rainstorm and 18.8% comes from rainstorm.
- The Euphrates river water is classified as fresh, slightly alkaline water, and very hard water, characterized by active ability of leaching in under saturation conditions with respect to the mineral phases of dolomite, calcite/aragonite, gypsum/anhydrite, and halite/sylvite. The different values of saturation indices confirm the variability of dissolution mechanisms for chloride, carbonate, sulfate, and mineral phases happened in Euphrates riverbeds and its catchment area. The nature and mechanism by which the saline waters originated (e.g., evaporation of river/saltwater beyond halite saturation, dissolution of halite, domestic wastewater) will control the Na/Cl ratios of the brine and consequently the bromide content of the salinized water.
- The results derived from water quality assessment indicate that there are no serious natural or industrial pollution cases, with absence sources of thermal pollution that has a serious impact on the biological diversity of the Euphrates water system.
- The results of the physico-chemical components found that their values were within their limits in a natural river environment and less than the prescribed limits for domestic use and human drinking purposes during rainy periods, and exceeded the desirable limit for TDS, Ca, and Mg, therefore classified as Fair water in samples collected before and after rainfall. Also, Euphrates river is of good class water within the safe recommended limits for animals drinking.
- Quality assessment of irrigation suitability indicated by Kelley index (KI), residual sodium carbonate (RSC), and sodium adsorption ratio (SAR), confirms that the water belongs to admissible and good quality class; therefore, river water is potable for irrigation and agricultural activities.
- According to the quality criteria of water for industrial purposes, Euphrates water can be used in the construction industry, low pressure boilers and cannot be used in high

pressure boilers employ. Also, the corrosivity ratio (CR) indicates that Euphrates water is unsafe (CR > 1) against metallic materials, especially when using in long distance transportation through metallic pipe lines.

- The Euphrates river is classified as healthy ecosystem and its water rated as good class for aquatic life according to the CCME water quality index.

Acknowledgements The authors thank the Department of Ecology, College of Applied Sciences-Hit at University Of Anbar (Iraq) for achieving this Research Project No. 16/5 on 15 Oct 2018.

Declarations

Conflict of interest The authors declared that there is no conflict of interest.

References

Al-Hamdani M, Al-Dulaymi A, Hussien B (2012) Sources of ions and trace elements in the water of Euphrates river from Qaem to Baghdadi (statistical study). Iraqi Bulltin of Geology and Mining 8:1811–4539

Al-Jabbari M, Hassen Q, Emad M (2002) National programme in the best used of water resources within Euphrates basin. Unpub. Study. Ministry of Agriculture, Baghdad, p 520

Al-Janabi M (2008) Qualitative and environmental study for Euphrates river from Dyer Elzor to Baghdadi, using chemical analysis and remote sensing. Thesis, Science College, Anbar University, Unpub (in Arabic)

Al-Sudani HI (2018) Calculating of groundwater recharge using meteorological water balance and water level fluctuation in Khan Al-Baghdadi area. Iraqi Journal of Science 59:349–359

Altoviski M (1962) Handbook of hydrogeology. Gosgeolitzdat, Moscow, USSR, p 614

Amiri V, Berndtsson R (2020) Fluoride occurrence and human health risk from groundwater use at the west coast of Urmia Lake, Iran. Arab J Geosci 13:1–23

Amiri V, Rezaei M, Sohrabi N (2014) Groundwater quality assessment using entropy weighted water quality index (EWQI) in Lenjanat, Iran. Environ Earth Sci 72:3479–3490

Amiri V, Sohrabi N, Dadgar MA (2015) Evaluation of groundwater chemistry and its suitability for drinking and agricultural uses in the Lenjanat plain, central Iran. Environ Earth Sci 74:6163–6176

Amiri V, Nakhaei M, Lak R, Kholghi M (2016) Assessment of seasonal groundwater quality and potential saltwater intrusion: a study case in Urmia coastal aquifer (NW Iran) using the groundwater quality index (GQI) and hydrochemical facies evolution diagram (HFE-D). Stoch Env Res Risk A 30:1473–1484

Amiri V, Kamrani S, Ahmad A, Bhattacharya P, Mansoori J (2020) Groundwater quality evaluation using Shannon information theory and human health risk assessment in Yazd province, central plateau of Iran. Environmental Science and Pollution Research p:1–23

Appelo CAJ, Postma D (2005) Geochemistry, groundwater and pollution, 2nd edn. Balkema, Rotterdam

Ayers R, Westcot D (1985) Water quality for agriculture, FAO irrigation and drain, Paper No. 29, Rev 1, Food and Agriculture Organization of the United Nations Rome p 1-109

Canadian Council of Minister of the Environment (CCME) (2001) Canadian water quality guidelines for the protection of aquatic life: CCME water quality index 1.0, Technical Report. Canadian Council of Ministers of the Environment Winnipeg MB, Canada

Chadha DK (1999) A proposed new diagram for geochemical classification of natural waters and interpretation of chemical data. Hydrogeol J 7(5):431–439

Collin's, A.G (1975) Geochemistry of oil field water. Development in Petroleum science-1, Holl-and p 496.

Crist MA, Lowry ME (1972) Groundwater resource of Natrona county Wyming. In: A study of the availability and chemical quality of groundwater, GS Water Supply paper 1897. US. Government printing office, Washington, p 92

Esmaeili-Vardanjani M, Rasa I, Amiri V, Yazdi M, Pazand K (2015) Evaluation of groundwater quality and assessment of scaling potential and corrosiveness of water samples in Kadkan aquifer, Khorasan-e-Razavi Province, Iran. Environ Monit Assess 187:53

Fayyadh AS, Bayan M, Hussien BM, Al-Hamdani MA, Salim SA, Mukhlef HN, Abed MA (2016) Hydrologic system of Euphrates river (spatial analyses) between Al-Qaem and Fallja. Iraqi Bulltin of Geology and Mining 12:1–118

Fitts C (2002) Groundwater science. Elsevier Science. Ltd, p 450

Golekar R, Baride M, Patil S (2014) Geomedical health hazard due to groundwater quality from Anjani-Jhiri River Basin, Northern Maharashtra, India. Int ResJ Earth Science 2:2321–2527

Guey-Shin S, Bai-You C, Chi-Ting C, Pei-Hsuan Y, Tsun-Kuo C (2011) Applying factor analysis combined with kriging and information entropy theory for mapping and evaluating the stability of groundwater quality variation in Taiwan. Int J Environ Res Public Health 8: 1084–1109

Helsel D, Hirsch R (2002) Statistical methods in water resources, chapter A3. Techniques of waterresources investigations of the US Geological Survey, Book 4

Hem, J., 1989; Study and interpretation of the chemical characteristics of natural water, 3rd. edition USGS Water Supply. Paper 2254, p 263.

Hussien BM, Faiyad AS (2016) Modeling the hydrogeochemical processes and source of ions in the groundwater of aquifers within Kasra-Nukhaib region (West Iraq). Int J Geosci 7:1156–1181

Issa IE, Al-Ansari N, Sherwany G, Knutsson S (2014) Expected future of water resources within Tigris-Euphrates rivers basin, Iraq. Journal of Water Resource and Protection 6:421–432

Jankowski J, Acworth RI (1997) Impact of debris flow deposits on hydrogeochemical process and the development of dry land salinity in the Yass River catchment, New South Wales Australia. Hydrogeol J 5:71–88

Johnes PJ (2007) Uncertainties in annual riverine phosphorus load estimation: impact of load estimation methodology, sampling frequency, baseflow index and catchment population density. J Hydrol 332: 241–258

Kamrani S, Rezaei M, Amiri V, Saberinasr A (2016) Investigating the efficiency of information entropy and fuzzy theories to classification of groundwater samples for drinking purposes: Lenjanat Plain, Central Iran. Environ Earth Sci 75:1370

Karanth KR (1989) Groundwater assessment development and management. Tata McGraw-Hill Publ. Com. Ltd, New Delhi, India

Kelley WP (1946) Permissible composition and concentration of irrigation waters. In: Proc. Amer. Soc. Civil Eng, p 607

Langmuir D (1997) Aqueous Environmental Geochemistry, Colorado School of Mines. Prentice Hall. Upper Saddle River, New Jersey p 07458,618

Lewen MC, King NJ (1971) Prospect for developing stockwater supplies from wells in north eastern. Car field county, Montana, GS Water Supply paper 1999-F,US. Government printing office, Washington 38

Littlewood IG, Marsh TJ (2005) Annual freshwater river mass loads from Great Britain, 1975–1994: estimation algorithm, database and monitoring network issues. J Hydrol 304:221–237

Masoumi SZ, Kazemi F, Oshvandi K, Jalali M, Esmaeili-Vardanjani A, Rafiei H (2016) Effect of training preparation for childbirth on fear of normal vaginal delivery and choosing the type of delivery among pregnant women in Hamadan, Iran: a randomized controlled trial. Journal of Family & Reproductive Health 10(3):115

Matthess G (1982) The properties of groundwater. In: Department of Environmental Science, vol 406. John Wiley and Sons Inc, New York

McKee JE, Wolf HW (1963) Water quality criteria: California State Water Quality Control Board Publication 548

Mitas L, Mitasova H (1999) Spatial interpolation. In: Longley PA, Godchild MF, Maguire DJ, Rhind DW (eds) Geographical information systems: principles, techniques, multivariate interpolation of precipitation 149, ß Blackwell Publishers Ltd. 2002. Management and Applications, New York, Wiley, p 481±92

Mullaney JR, Lorenz DL, Arntson AD (2009) Chloride in groundwater and surface water in areas underlain by the Glacial Aquifer System, Northern United States National Water-Quality Assessment Program, Scientifc Investigations Report. U.S. Geological Survey, Reston, Virginia, pp 2009–5086

Nakhaei M, Amiri V, Rezaei K, Moosaei F (2015) An investigation of the potential environmental contamination from the leachate of the Rasht waste disposal site in Iran. Bull Eng Geol Environ 74:233–246

Nakhaei M, Dadgar MA, Amiri V (2016) Geochemical processes analysis and evaluation of groundwater quality in Hamadan Province, Western Iran. Arab J Geosci 9:384

Paliwal KV (1967) Effects of gypsum application on the quality of irrigation water; The Madras Agr. Jour. 59:646–647

Parkhurst DL, Appelo CAJ (1999) User's Guide to PHREEQC (version 2)-a computer program for speciation, batch-reaction, one-dimensional transport, and inverse geochemical calculations. USGS Water-Resources Investigations Report 99-4259. Petalas, C.P.

Rana R, Ganguly R, Gupta AK (2018) Indexing method for assessment of pollution potential of leachate from non-engineered landfill sites and its effect on ground water quality. Environ Monit Assess 190:46

Sami K (1992) Recharge mechanisms and geochemical processes in a semi-arid sedimentary basin. Eastern Cape, South Africa, Journal of Hydrology 139:27–48

Schoeller H (1977) Geochemistry of groundwater. In: Groundwater Studies- An International Guide for Research and Practice, vol 15. UNESCO, Paris Ch, pp 1–18

Sessikian V, Mohammed B (2007) Stratigraphy of the Iraqi western desert. IBGM, ISSN 1811-4639, Special ISSUE, SCGSM, P51-125

Shafer M, Overdier J, Hurley J, Armstrong D, Webb D (1997) The influence of dissolved organic carbon, suspended particulates, and hydrology on the concentration, partitioning and variability of trace metals in two contrasting Wisconsin watersheds (U.S.A.). Chem Geol 136:71–97

Sharma A, Ganguly R, Gupta AK (2020) Impact assessment of leachate pollution potential on groundwater: an indexing method. J Environ Eng 146:05019007

Shelton L (1994) Field guide for collecting and processing stream-water samples for the National Water Quality Assessment Program. USGS Open-File Report 94-455. Sacramento, California. US.Geological Survey. NAWQA Field Technical Support . Placer Hall 6000 J Street Sacramento, Ca. 95819-6129

Siegel F (2002) Environmental geochemistry of potentially toxic metals. Springer, Berlin, p 230

Sohrabi N, Kalantari N, Amiri V, Nakhaei M (2017) Assessing the chemical behavior and spatial distribution of yttrium and rare earth elements (YREEs) in a coastal aquifer adjacent to the Urmia Hypersaline Lake, NW Iran. Environ Sci Pollut Res 24:20502–20520

Stumm W, Morgan JJ (1981) Aquatic chemistry. John Wiley & Sons, 1981

Todd DK, Mays L (2005) Ground water hydrology, John Wiley and Son, Inc, Toppan company (LTD), New York

Tyracek J (1981) Euphrates river terraces. J Geol Soc Iraq 14:1–81

US Environmental Protection Agency (2002) Drinking water advisory consumer acceptability advice and health effects analysis on sodium. Office of Water, Washington DC p 34

US Salinity Laboratory Staff (USSLS) (1954) Diagnosis and improvement of saline and alkali soils. U.S. Department of Agriculture Hand Book p 160

Vasistha, Prachi, and Rajiv Ganguly (2020a) Assessment of spatio-temporal variations in lake water body using indexing method Environ Sci Pollut Res p 1-20.

Vasistha P, Ganguly R (2020b) Water quality assessment of natural lakes and its importance: an overview. Proceedings, Materials Today

Walling DE, Webb BW (1985) Estimating the discharge of contaminants to coastal waters by rivers: some cautionary comments. Mar Pollut Bull 16:488–492

Walton WC (1970) Groundwater resource evaluation. Mc Graw-Hill series p 664

WHO (2011) Guidelines for drinking water quality, 4th edn. World Health organization, Geneva

Wilde, D. Franceska (2005) Handbooks for water resources investigations. National Field Manual for the Collection of Water Quality Data, Chapter- A1, A2, A3, A4, A5, Version 2.0 . USGS publication series, Techniques of Water-Resources Investigations, TWRI Book 9

Zhu GF, Su YH, Feng Q (2008) The hydro geochemical characteristics and evolution of groundwater and surface water in the Heihe River Basin, northwest China. Hydrogeol J 16:167–182